Reaction Chemistry & Engineering

Minimization of Pt-electrocatalyst deactivation in CO_2 reduction using polymer electrolyte cell

Journal:	*Reaction Chemistry & Engineering*
Manuscript ID	RE-ART-03-2020-000083.R1
Article Type:	Paper
Date Submitted by the Author:	30-Mar-2020
Complete List of Authors:	Matsuda, Shofu; Nagaoka University of Technology, Department of Materials Science and Technology Tamura, Shigehisa; Nagaoka University of Technology, Department of Materials Science and Technology Yamanaka, Shota; Nagaoka University of Technology, Department of Materials Science and Technology Niitsuma, Yuuki; Nagaoka University of Technology Sone, Yoshitsugu; Japan Aerospace Exploration Agency Sagamihara Campus; SOKENDAI Umeda, Minoru; Nagaoka University of Technology, Materials Science and Technology, Faculty of Engineering

ARTICLE

Minimization of Pt-electrocatalyst deactivation in CO_2 reduction using polymer electrolyte cell

Received 00th January 20xx,
Accepted 00th January 20xx

DOI: 10.1039/x0xx00000x

Shofu Matsuda,[a] Shigehisa Tamura,[a] Shota Yamanaka,[a] Yuuki Niitsuma,[a] Yoshitsugu Sone [b] and Minoru Umeda *[a]

Diluted CO_2 feeding was recently reported to efficiently generate CH_4 at the theoretical Pt electrode potential, however, the reaction was easily deactivated. To solve this problem, we investigated the reaction/deactivation mechanism to produce CH_4 from CO_2 electroreduction. Using a polymer electrolyte single cell containing a Pt/C catalyst, CO_2 was reduced to CH_4 without overpotential by simply controlling the CO_2 feed concentration. The CH_4 synthesis proceeded if the Pt-CO/Pt-H ratio formed on the Pt-catalyst surface was 1:11 or higher. The deactivation of the CH_4 generating reaction also depends on the Pt-CO/Pt-H ratio (the ratio does not satisfy 1:11 or higher). The optimum Pt-CO/Pt-H ratio to produce CH_4 was 1:18. Furthermore, we achieved 86% recovery of CH_4 activity by sweeping the deactivated Pt surface on the cathode up to 0.3 V where the CO_2/Pt-CO redox reaction occurred simultaneously. As a result, an efficient less energy-intensive reactivation reaction that we defined as poisoning-elimination method was established. Overall, this work demonstrated that the application of a polymer electroryte cell together with a low concentration of CO_2 is effective to minimize the Pt-electrocatalyst deactivation.

Introduction

Many international organizations including the United Nations have eagerly stated that reducing the growing atmospheric CO_2 is an urgent task to prevent global warming.[1] Regarding CO_2 reduction, recent carbon-capture research and development aims not only at CO_2 storage but also at the utilization and chemical conversion of the captured CO_2.[2-4] This concept is referred to as carbon capture and utilization (CCU). However, CO_2 fixation and chemical reduction is quite difficult because CO_2 is the stable most oxidized form of carbon. One promising technology is methanation or the Sabatier reaction using catalysts ($CO_2 + 4\ H_2 \rightarrow CH_4 + 2\ H_2O$), but it is conducted with a batch reaction which requires a temperature of several hundred °C.[5,6] Hence, it is less attractive for large-scale CO_2 processing. On the other hand, electrochemical CO_2 reduction is currently receiving great attention. When employing a Cu electrocatalyst as a cathodic electrode, hydrocarbons can be obtained with a current efficiency of approximately 60%.[7] However, its energy efficiency is extremely low because the reactions proceed with a large overpotential (ca. 1.4 V).[7,8]

To solve the issues regarding the CO_2 electroreduction, many electrode materials were investigated to realize CCU, however, without success. The electrolysis conditions require a negligible overpotential, high faradaic efficiency and a high reaction selectivity. The former two are inevitable to achieve a high energy efficiency, and the latter is necessary to convert CO_2 to valuable chemicals. In the case of the earlier mentioned Cu electrode, a high faradaic efficiency of 60% results in a high overpotential of 1.4 V, producing CH_4, C_2H_4 and H_2 at low selectivity. The same tendencies are observed with other electrode materials such as Au or Ag.[9-14] Consequently, an ideal electrolysis-based CCU process is quite difficult to realize presently.

To improve the situation, it seems to be advantageous to utilize a Pt electrocatalyst for CO_2 reduction[15] to efficiently generate Pt-CO[16-18] close to the theoretical electrode potential. Thus far, a further reduction of Pt-CO to obtain valuable chemicals seems to be difficult, because the strong Pt-CO bond deactivates and prevents any subsequent reactions.[19] Recently, we computationally demonstrated the CO_2 adsorption on Pt,[20] and observed a 50% Pt-CO generation efficiency[21] and a 0.4% CH_4 production efficiency.[22] The CO_2 reduction took place at the Pt-loaded carbon (Pt/C) surface of a membrane electrode assembly (MEA) close to the theoretical electrode potential.[22]

A closer look at the chemical structure of the intermediate, Pt-CO, and the CH_4 product, revealed that the Pt-CO reduction apparently required an H source. Interestingly, in some aprotic electrolytes of non-aqueous solutions,[23,24] molten salts[25] and solid oxide electrolytes,[26] the major CO_2 electroreduction product is CO. In the case of water–acetonitrile (AN) mixed solutions, the CO_2 reduction products at the Pt electrode change from oxalic acid and formic acid to H_2 with increasing water/AN ratio.[27] In addition, the faradaic efficiency of the products is almost identical. This strongly suggests

[a] Department of Materials Science and Technology, Faculty of Engineering, Nagaoka University of Technology, 1603-1, Kamitomioka, Nagaoka, Niigata 940-2188, Japan
[b] Institute of Space and Astronautical Science, Japan Aerospace Exploration Agency, 3-1-1 Yoshinodai, Chuo-ku, Sagamihara, Kanagawa 252-5210, Japan

† Electronic Supplementary Information (ESI) available: [details of any supplementary information available should be included here]. See DOI: 10.1039/x0xx00000x

a mechanism that Pt-CO reacts with H_2O in the mixed H_2O–AN solution. Anyway, a large overpotential still remained.

Very recently, we reported a novel strategy in which Pt-CO collaborates with Pt-H using the MEA, to selectively produce CH_4 with a negligible competing H_2 generation and, more importantly, at potentials close to the theoretical electrode potential of the reaction. To form an appropriate Pt-CO/Pt-H ratio for CH_4 generation, we changed the CO_2 partial pressure by diluting with Ar. It improved the CO_2 electroreduction without overpotential and at high selectivity.[28] However, deactivation during continuous operation was observed.

According to this situation, we have focused our attention on the deactivation phenomenon in terms of Pt surface poisoning. In the present study, Pt/C has been employed as an electrocatalyst in combination with a polymer electrolyte membrane in a flow electrolyzer. First, we describe the reaction mechanism of Pt-CO/Pt-H to generate CH_4 with high selectivity close to the theoretical potential. Next, the deactivation process is discussed based on the reaction mechanism. Finally, a method to eliminate poisoning was established by controlling the Pt-CO and Pt-H formation.

Experimental

Preparation of a Pt/C single cell

A CO_2 electrolysis cell was prepared using methods outlined previously.[28,29] In short, we prepared a polymer electrolyte single cell equipped with a Nafion-based MEA containing 46.2 wt% Pt/C as working, counter, and reference electrode (WE, CE, and RE). The apparent surface area and the loaded Pt amount of WE were 9 cm^2 and 1.0 mg/cm^2, respectively. The Nafion 117 membrane with a size of 6 × 6 cm (0.180 mm thick) was purchased from DuPont. The Pt/C powder (TEC10E50E) was obtained from Tanaka Kikinzoku Kogyo Co., Ltd.

CO_2 electroreduction

The prepared Pt/C single cell was connected to an FCG-20S polymer electrolyte fuel cell power generation unit (ACE, Inc.), an HA-310 potentiostat/galvanostat (Hokuto Denko), an HB-104 function generator (Hokuto Denko), and an HE-151 electrometer (Hokuto Denko). After the cell temperature was set to 40°C, a fully humidified Ar/CO_2 gas (CO_2 concentration: 0, 4, 5, 6, 7, 10, 20, 50, and 100 vol.%) was supplied to the WE at a flow rate of 50 cm^3/min and a pressure of 1 atm. Fully humidified H_2 gas at 50 and 10 cm^3/min was supplied to the CE and RE, respectively. Cyclic voltammetry (CV) was performed at the potential range between 0.08 V and 1.0 V at a scan rate of 10 mV/s. Additionally, the same type CV was measured after potential holding at the various WE potentials and holding times at 4 and 5 vol.% CO_2. Linear sweep voltammetry for positive direction between 0.08 to 0.7 V was conducted at the slow scan rate of 0.1 mV/s. In order to analyze the CO_2 electroreduction product in real time, the WE exhaust gas was introduced directly into a JMS-Q1050GC quadrupole mass spectrometer (MS; JEOL). During in-line MS analysis, the time delay in the product detection was corrected with reference to H_2 detection.[28,30] The ionization energy was 16 eV. All the potentials are shown with reference to the reversible hydrogen electrode (RHE).

Results and Discussion

CO_2-concentration dependence of CH_4 yield at electrode potential outside the competing H_2 production

Fig. 1 shows cyclic voltammograms and MS signals at *m/z* 2 (H_2) and 15 (CH_3^+) at 0, 5, and 100 vol.% CO_2. The *m/z* 15 is a fragment of CH_4 and is not affected by oxygen derived from CO_2 and H_2O. Comparing the voltammograms using 5 vol.% and 100 vol.% CO_2, it was confirmed that the magnitudes of the anodic current peaks between 0.08–0.35 V (H desorption)[21,31] and 0.5–0.7 V (CO desorption)[21,31] are different. Consequently, *m/z* 15 as a product was remarkably detected in the range of 0.2–0.08 V using 5 vol.% CO_2. Here, the detected *m/z* 15 is attributed to CH_4 generated from CO_2 reduction, as shown in Fig. S1 in the Electronic Supplementary Information (ESI)†. Considering the theoretical potential of the CO_2 reduction to CH_4 in acidic solution or acidic medium (0.169 V vs. RHE)[32], it should be noted that CO_2 was reduced to CH_4 without overpotential. As expected, the *m/z* 15 signal was not detected using 0 vol.% CO_2, as shown in Fig. 1(a). On the other hand, the *m/z* 2 signal appeared below 0.1 V at all CO_2 concentrations used. Therefore, this system enables the CO_2 electroreduction into CH_4 outside the competing H_2 generation. So far as known, no product was obtained from CO_2 reduction (only H_2 evolution occurred) at a Pt electrocatalyst in aqueous media.[33] However, the selective CH_4 generation on a Pt electrocatalyst was achieved in this work using a polymer electrolyte cell under a diluted CO_2 condition.

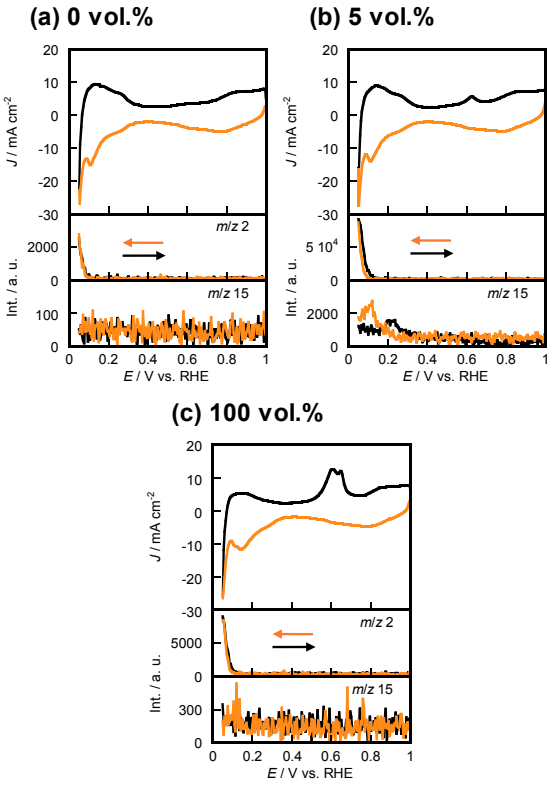

Fig. 1. Cyclic voltammograms (top) and MS signal intensities at *m/z* 2 (middle) and 15 (bottom) in the single cell incorporating Pt/C at the cell temperature of 40°C under CO_2 concentrations of (a) 0 vol.%, (b) 5 vol.%, and (c) 100 vol.%.

We then calculated the dependences of the CH_4 amount generated from CO_2 reduction and the faradaic CH_4 generation efficiency at 0.2–0.1 V on CO_2 concentration, as shown in Fig. 2 using Eq. 1.[32] A calibration curve (CH_4 amount vs. *m/z* 15 intensity) was also

obtained at a flow rate of 50 cm^3/min using a CH_4 gas (purity: 99.999%) diluted in Ar.

$CO_2 + 8\ H^+ + 8\ e^- \rightarrow CH_4 + 2\ H_2O$ (1)

We observed the CH_4 amount of approximately 40 nmol and an efficiency of about 3% at 4–6 vol.% CO_2 feeding, but a negligible amount of CH_4 was generated at 100 vol.% CO_2, which corresponds well previously reported trends.[28] In other words, the CO_2 concentration is a significant control factor to enhance CH_4 formation. These results show that the optimum CO_2 concentration for efficient CH_4 production is 4–6 vol.%.

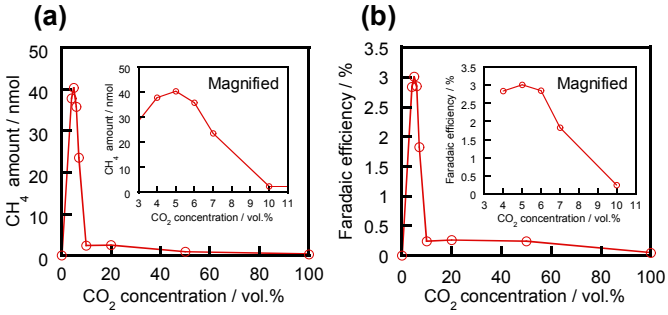

Fig. 2. CO_2-concentration dependence of (a) CH_4 amount and (b) faradaic CH_4 production efficiency from CO_2 reduction on a Pt electrocatalyst at a flow rate and apparent electrode-surface area of 50 cm^3/min and 9 cm^2, respectively.

CO_2 reduction depending on Pt-CO/Pt-H ratio

We considered the reason why efficient CH_4 generation occurs at low CO_2 concentrations (4–6 vol.%). Fig. 3(a) shows cyclic voltammograms at various CO_2 concentrations. Importantly, the magnitude of the H-desorption current peak at 0.08–0.35 V increased, but that of the CO-desorption current peak at 0.5–0.7 V decreased at low CO_2 concentration. This indicated that the of Pt-CO/Pt-H formation ratio was successfully controlled by diluting the CO_2 feed.

Then, we calculated the coulombic charges of the two anodic peak currents, followed by determination of the Pt-CO/Pt-H ratio formed on the Pt-catalyst surface, taking into account the number of electrons for each oxidation reaction. The CO-desorption and H-desorption reactions are two-electron and one-electron reactions, respectively.[34] Hence, the Pt-CO/Pt-H ratio was determined by the following formula:

Pt-CO/Pt-H ratio = $(Q_{CO} \div 2) / (Q_H \div 1)$ (2)

where Q_{CO} and Q_H mean coulombic charges of CO desorption and H desorption, respectively. Fig. 3(b) shows the dependence of the faradaic CH_4 generation efficiency on the Pt-CO/Pt-H ratio. A threshold of CH_4 generation is observed at the of Pt-CO and Pt-H ratio of approximately 1:11. According to our previous report[28], this CH_4-generating reaction follows a Langmuir-Hinshelwood mechanism represented by the following equation:

Pt-CO + 6 Pt-H→ $CH_4 + H_2O$ + 7* (3)

where * means an active site on the Pt surface. Therefore, CH_4 is theoretically produced when the Pt-CO/Pt-H ratio at the Pt surface becomes 1:6. However, it was experimentally revealed that the Pt-CO/Pt-H ratio needs to be 1:11, preferably 1:14 or more to produce CH_4 from CO_2 reduction. Moreover, the highest faradaic efficiency (3.0%) was obtained at the Pt-CO/Pt-H ratio of 1:18 as shown in Fig. 3(b).

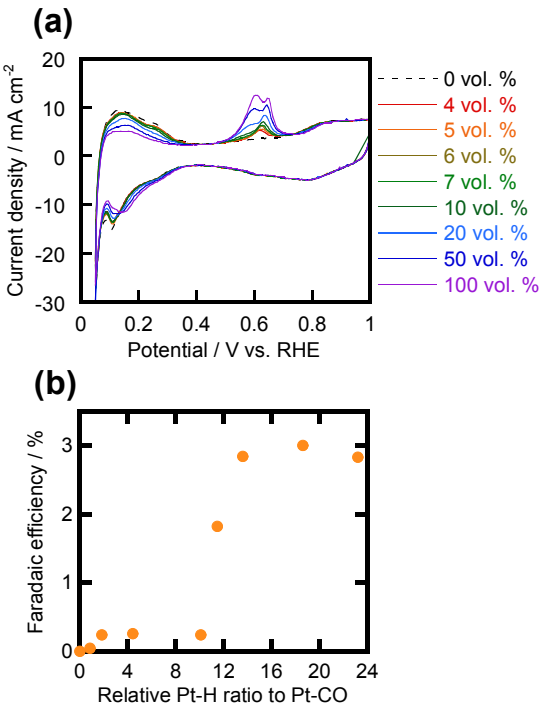

Fig. 3. (a) Cyclic voltammograms of the WE (Pt/C electrocatalyst) at 40°C under various CO_2 concentrations. (b) Faradaic CH_4 generation efficiency during CO_2 reduction (as shown in Fig. 2) as a function of the relative Pt-H ratio to Pt-CO formed on the catalyst surface and calculated from the coulombic charges of two anodic peaks in the voltammograms shown in (a). The CO_2 concentrations in the left plot are shown in the order 0, 100, 50, 20, 10, 7, 6, 5, 4 vol.%.

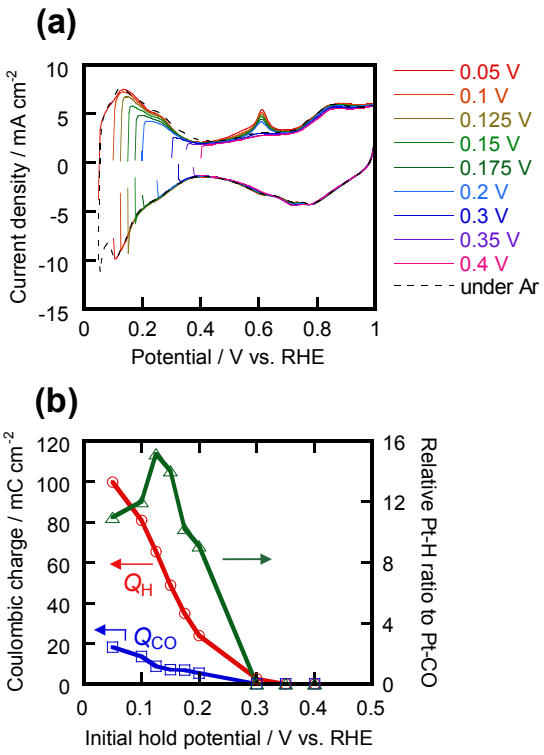

Fig. 4. (a) Cyclic voltammograms at each initial hold potential for 17 s at 5 vol.% CO_2. (b) Dependence of coulombic charge of oxidation peak currents (Q_H between 0.08-0.35 V

and Q_{CO} between 0.5-0.7 V in the voltammograms shown in (a)) and dependence of the relative Pt-H ratio to Pt-CO on initial hold potential.

To evaluate the effect of electrode potential on CH_4 generation, cyclic voltammograms were measured at 5 vol.% CO_2, in which a 17 s potential hold at the various electrode potentials was performed before each potential sweep, as shown in Fig. 4(a). As a result, both the oxidation peak currents for H desorption and CO desorption decreased as the initial hold potential changed to the positive direction. Fig. 4(b) shows the dependence of the coulombic charges of the oxidation currents Q_H and Q_{CO} on the initial hold potential. Q_H and Q_{CO} also decreased as the initial hold potential changes to the positive direction. The potential dependence of the Pt-CO/Pt-H ratio is also presented in Fig. 4(b). It should be noted that the ratio was 1:11 or higher in the potential range for CH_4 generation (0.18–0.05 V). In detail, the relative Pt-H ratio to Pt-CO increased at potentials ranging from 0.3 V to 0.15 V, and then it decreased in the range of 0.15 V to 0.05 V (Fig. 4(b)). Because the ratio was highest at the value of ca. 1:15 at the potential of 0.15 V, this potential would be most suitable for efficient CH_4 production. Overall, the quantitative dependence of the Pt-CO/Pt-H ratio on both CO_2 concentration and electrode potential was elucidated in this section.

Deactivation mechanism of CH_4 generation

In our previous study,[28] the CH_4 generation from CO_2 reduction using Pt electrocatalysts quickly decreased within 30 s when the potential was held at 0.1 V. In the following, we discuss the deactivation of the CH_4 production associated with the Pt-CO/Pt-H ratio. As shown in Fig. 5(a), the *m/z* 15 signal corresponding to CH_4 formation was observed between 0.2–0.08 V when CV was performed at 5 vol.% CO_2. This would be explained by the relative Pt-H ratio to Pt-CO larger than 11 formed on Pt-catalyst surface, as shown in Fig. 4(b). However, when the potential was held for 150 s at 0.1 V, which results in a Pt-CO/Pt-H ratio of 1:11 or more, the CH_4 production decreased over time and stopped within approximately 50 s, as shown in Fig. 5(b). Afterward, CH_4 production was reinstalled when the electrode potential was swept from 0.1 V for positive direction, as shown in Fig. 5(c). This reactivated the CH_4 formation by cleaning the catalyst surface applying a potential between 0.5–1.0 V. In this potential range, an oxidation current was observed, which contributed to reset the electrode surface.[35] Comparing Figs. 5(a) to 5(c), the anodic peak current at 0.5–0.7 V (CO desorption) in Fig. 5(c) was larger than that in Fig. 5(a). Therefore, it is apparent that the CH_4 deactivation observed for the Pt electrocatalyst in Fig. 5(b) is attributed to CO poisoning.

In order to confirm the deactivation mechanism, we then investigated the dependence of the Pt-CO/Pt-H ratio on the holding time at 0.1 V. As shown in the voltammograms of Fig. 6(a), the anodic CO-desorption current at 0.5–0.7 V became larger as the holding time increased, but the anodic H-desorption current at 0.1–0.35 V for each holding time was similar. The formation ratio of Pt-CO/Pt-H was according to Fig. 6(a), 1:14, 1:10, and 1:6.4 at 0.1 V-holding times of 0, 19, and 49 s, respectively, as shown in Fig. 6(b). The result of Fig. 5(b), where CH_4 production decreased over time can be explained by a decrease in the ratio of Pt-H to Pt-CO. The CH_4 formation stopped within 50 s because the ratio decreased to below 11, according to Fig. 3(b). Therefore, the deactivation of the CH_4 generation occurs when the Pt-CO/Pt-H does not satisfy 1:11 or higher. In other words, constant CH_4 production could be achieved with a method that enables to maintain a Pt-CO/Pt-H ratio of 1:11 or higher at the Pt-catalyst surface. Based on the results in this section, the quantitative relation between deactivation and the ratio of Pt-CO/Pt-H was determined and the CH_4-regeneration phenomenon demonstrated.

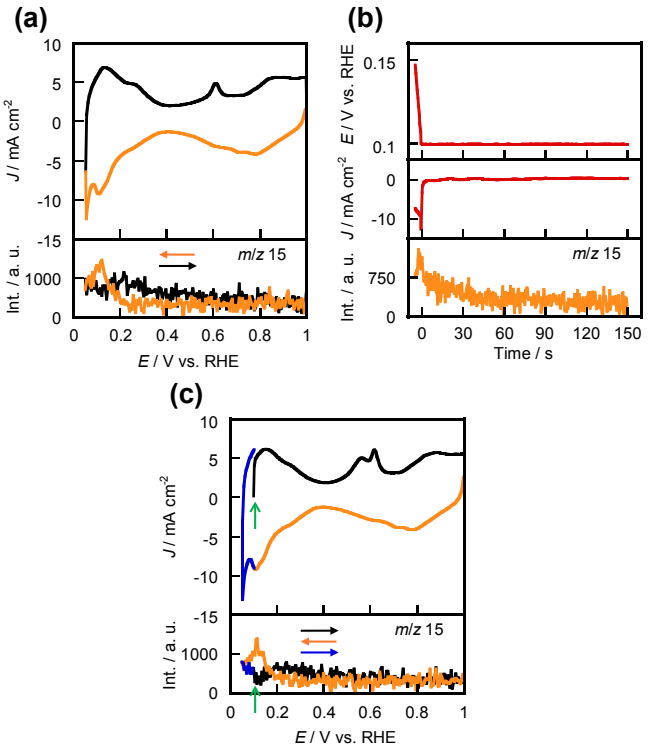

Fig. 5. Response of the *m/z* 15 signal (bottom) for (a) a potential sweep between 0.08 V and 1.0 V, for (b) a potential hold at 0.1 V for 150 s, and for (c) a potential sweep from 0.1 V for positive direction after a potential hold at 0.1 V for 150 s, at a CO_2 concentration of 5 vol.%. Green arrows mean a start potential (0.1 V) for the potential sweep and in-line MS.

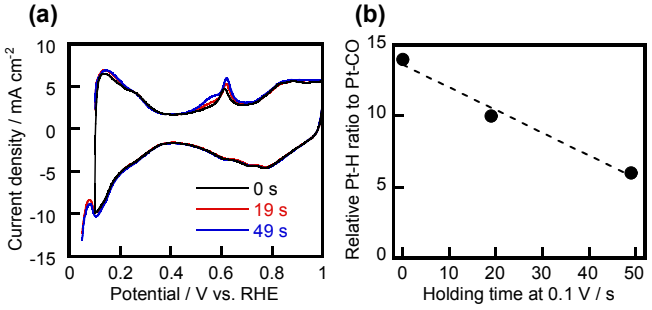

Fig. 6. (a) Cyclic voltammograms after potential holding at 0.1 V at specific time periods for 5 vol.% CO_2. (b) Dependence of the relative Pt-H ratio to Pt-CO on the hold time at 0.1 V.

Poisoning elimination treatment based on the deactivation mechanism

Although we achieved CH_4 regeneration by sweeping the electrode surface at 0.5–1.0 V in the previous section, this way to eliminate poisoning is energy-intensive and disadvantageous for practical applications. To overcome this obstacle, we focused our attention on optimizing the potential limit for the anodic sweep.

First, we investigated the onset potential of Pt-CO regarding the CO_2 oxidation reaction. Fig. 7(a) shows the linear sweep voltammogram (LSV) at slow scan rate (under quasi-stationary

condition) at 4 vol.% CO_2. Compared to the LSV at 0 vol.% CO_2, the onset potential for the Pt-CO oxidation to CO_2 was 0.3 V.

Subsequently, we investigated the onset potential of CO_2 for the Pt-CO reduction reaction. Based on the cyclic voltammograms shown in Fig. S2 (ESI†), we calculated the coulombic charge of the anodic CO-desorption current (at 0.5–0.7 V in Fig. S2, ESI†), and plotted it as a function of initial hold potential, displayed in Fig. 7(b). The coulombic charge decreased with a positive shift at the hold potential and disappeared at 0.35 V. Therefore, we determined that the onset potential of CO_2 to Pt-CO is 0.35 V.

Based on the results of the onset-potential investigations, the CO_2/Pt-CO redox reaction occurred simultaneously in the potential range of 0.3 V to 0.35 V. In other words, the CO-adsorption state on the Pt surface can be reversed (CO poisoning can be eliminated) at that potential range. Fig. 7(c) shows the response of the *m/z* 15 (CH_4 generation) signal for the potential sweep on the positive side up to 0.3 V after deactivation, presented in Fig. 5(b). Remarkably, CH_4 formation was observed at 0.2–0.08 V on the negative scan. Thus, the regeneration of the CH_4 production (poisoning elimination treatment) was achieved at lower energies compared to cleaning the catalyst surface at 0.5–1.0 V.

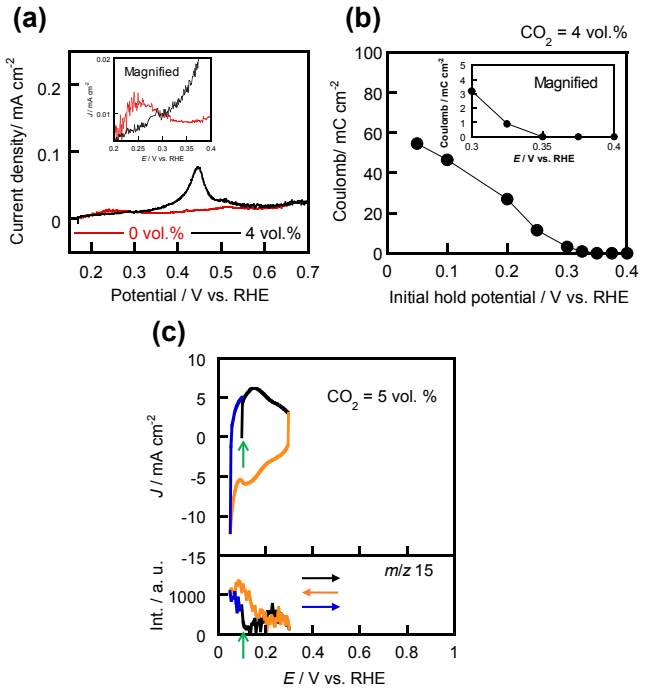

Fig. 7. (a) Linear sweep voltammogram for positive direction at 0.08–0.7 V at the scan rate of 0.1 mV/s at 0 and 4 vol.% CO_2. (b) Dependence of the coulombic charge derived from CO desorption on the initial hold potential for 5 min at 4 vol.% CO_2 (calculated from Fig. S2, ESI†). (c) Cyclic voltammogram (top) and response of the *m/z* 15 signal (bottom) for a potential sweep at 0.1 V for positive direction at 10 mV/s after a potential hold of 150 s at 0.1 V, at 5 vol.% CO_2. The potential limit for the anodic scan was 0.3 V. Green arrows determine the start potential (0.1 V) for CV and in-line MS.

To evaluate the regeneration of CH_4 formation quantitatively, we employed the evaluation parameter of recovery, which is defined by the following equation:

$$\text{Recovery}\ (\%) = \frac{\text{Amount of CH}_4\ \text{regenerated at 0.1 V}}{\text{Amount of CH}_4\ \text{generated at 0.1 V in Fig. 5a}} \times 100. \quad (4)$$

Each CH_4 amount was obtained using Eq. 1 and the calibration curve (CH_4 amount vs. *m/z* 15 intensity). As shown in Table 1, the recovery of CH_4 production related to Figs. 5(c) and 7(c) was as high as 85% compared to the initial CH_4 amount produced on the Pt electrocatalyst (Fig. 5(a)). Furthermore, the recovery regarding Figs. 5(c) and 7(c) was similar. Significantly, the recovery with regards to Fig. 7(c) is higher than that (~70%) obtained for a method utilizing a square-wave potential modulation between 0.1 V and 0.3 V, reported in our previous paper[28]. It is considered that the Pt-CO/Pt-H ratio for the potential sweep was close to 1:18 compared to that for the square-wave potential modulation. Indeed, the Pt-CO/Pt-H ratio restored was close to 1:17 after the potential sweep, though the ratio was 1:2.2 regarding Fig. 5(b), as shown in Fig. S3, ESI†. Therefore, these results strongly indicate that the reversal of the poisoning using an anodic potential sweep up to 0.3 V is energy-efficient and effective to regenerate CH_4 formation from CO_2 reduction using a Pt/C electrocatalyst. Overall, it was demonstrated in this section with regards to the CO_2/Pt-CO equilibrium condition and the Pt-CO/Pt-H ratio that the activity of Pt was restored with a less energy-intensive process. Alternative approaches to eliminate poisoning are considered.[36]

In fact, active electrocatalysts for CO_2 reduction are still very limited today (essentially, only to Cu) despite extensive studies for several decades,[8,23,37-40] and hence many researchers are looking for new strategies or concepts for developing more active catalysts and its operation system. The present work aimed to find ways to improve catalytic activities through fundamental mechanistic studies and succeeded in significantly improving the activity of Pt catalyst, although it is still not sufficient for practical applications, or scale-up. Based on the results in this study, a scaled-up periodic CH_4 generation would be possible if the stacked polymer electrolyte cells can be designed so that perform CH_4 generation and poisoning minimization alternately while supplementing the current.

Table 1. Various methods of CH_4 generation recovery (Fig. 5(c) and Fig. 7(c)).

Operation	Recovery / %
Fig. 5(c)	85.0
Fig. 7(c)	86.0

Conclusions

A polymer electrolyte single cell equipped with a membrane electrode assembly containing a Pt/C electrocatalyst was fabricated, and the reaction/deactivation mechanism of CH_4 generation from CO_2 reduction investigated. The highlights of our study are summarized as follows. CH_4 production reaction with an efficiency of about 3% proceeded at a more positive electrode potential than that of the H_2 evolution (without overpotential) by diluting the CO_2 feed. A Pt-CO/Pt-H ratio of 1:11 or more was required on the Pt surface for CH_4 generation. The deactivation of the CH_4 generation occurred when the Pt-CO/Pt-H does not satisfy 1:11 or higher. The CO_2/Pt-CO redox reaction occurred simultaneously in the potential range between 0.3 V and 0.35 V. An effective less energy-intensive regeneration of CH_4 production was demonstrated. These findings could benefit catalyst/process designs for effective CO_2 electroreduction not only related to Pt but also Cu, Au, and Ag catalysts.

Conflicts of interest

There are no conflicts to declare.

Acknowledgements

This work was supported by the Japan Science and Technology Agency (JST) through the Advanced Catalytic Transformation Program for Carbon Utilization (ACT-C, Grant Number JPMJCR12Y4) and by JSPS KAKENHI Grant Number JP15555941.

Notes and references

1. The United Nations Climinate Change Online, https://unfccc.int/, (accessed February 2020).
2. M. Peters, B. Köhler, W. Kuckshinrichs, W. Leitner, P. Markewitz and T. E. Müller, *ChemSusChem*, 2011, **4**, 1216.
3. Z.-Z. Yang, L.-N. He, J. Gao, A.-H. Liu and B. Yu, *Energy Environ. Sci.*, 2012, **5**, 6602.
4. M. Bui, C. S. Adjiman, A. Bardow, E. J. Anthony, A. Boston, S. Brown, P. S. Fennell, S. Fuss, A. Galindo, L. A. Hackett, J. P. Hallett, H. J. Herzog, G. Jackson, J. Kemper, S. Krevor, G. C. Maitland, M. Matuszewski, I. S. Metcalfe, C. Petit, G. Puxty, J. Reimer, D. M. Reiner, E. S. Rubin, S. A. Scott, N. Shah, B. Smit, J. P. M. Trusler, P. Webley, J. Wilcox and N. M. Dowell, *Energy Environ. Sci.*, 2018, **11**, 1062.
5. X. Wang, H. Shi, J. H. Kwak and J. Szanyi, *ACS Catal.*, 2015, **5**, 6337.
6. P. Panagiotopoulou, *Appl. Catal., A*, 2017, **542**, 63.
7. Y. Hori, I. Takahashi, O. Koga and N. Hoshi, *J. Phys. Chem. B*, 2002, **106**, 15.
8. M. Gattrell, N. Gupta and A. Co, *J. Electroanal. Chem.*, 2006, **594**, 1.
9. H. Mistry, R. Reske, Z. Zeng, Z.-J. Zhao, J. Greeley, P. Strasser and B. R. Cuenya, *J. Am. Chem. Soc.*, 2014, **136**, 16473.
10. W. L. Zhu, R. Michalsky, Ö. Metin, H. Lv, S. Guo, C. J. Wright, X. Sun, A. A. Peterson and S. Sun, *J. Am. Chem. Soc.*, 2013, **135**, 16833.
11. A. Dutta, C. E. Morstein, M. Rahaman, A. C. López and P. Broekmann, *ACS Catal.*, 2018, **8**, 8357.
12. H. Wang, Z. Han, L. Zhang, C. Cuia, X. Zhua, X. Liu, J. Han and Q. Ge, *J. CO_2 Util.*, 2016, **15**, 41.
13. F. Köleli, T. Atilan, N. Palamut, A. M. Gizir, R. Aydin and C. H. Hamann, *J. Appl. Electrochem.*, 2003, **33**, 447.
14. K. Nakata, T. Ozaki, C. Terashima, A. Fujishima and Y. Einaga, *Angew. Chem. Int. Ed.*, 2014, **53**, 871.
15. J. Giner, *Electrochim. Acta*, 1963, **8**, 857.
16. B. Beden, A. Bewick, M. Razaq and J. Weber, *J. Electroanal. Chem.*, 1982, **139**, 203.
17. T. Iwashita, F. C. Nart, B. Lopez and W. Vielstich, *Electrochim. Acta*, 1992, **37**, 2361.
18. S. Taguchi, A. Aramata and M. Enyo, *J. Electroanal. Chem.*, 1994, **372**, 161.
19. M. T. M. Koper and R. A. van Santen, *J. Electroanal. Chem.*, 1999, **476**, 64.
20. S. Matsuda, T. Mukai, S. Sakurada, N. Uchida and M. Umeda, *New J. Chem.*, 2019, **43**, 13717.
21. S. Shironita, K. Karasuda, K. Sato and M. Umeda, *J. Power Sources*, 2013, **240**, 404.
22. Y. Niitsuma, K. Sato, S. Matsuda, S. Shironita and M. Umeda, *J. Electrochem. Soc.*, 2019, **166**, F208.
23. Y. Hori, *Mod. Aspect. Electrochem.*, 2008, **42**, 89.
24. B. A. Rosen, A. Salehi-Khojin, M. R. Thorson, W. Zhu, D. T. Whipple, P. J. A. Kenis and R. I. Masel, *Science*, 2011, **334**, 643.
25. D. Chery, V. Lair and M. Cassir, *Electrochim. Acta*, 2015, **160**, 74.
26. V. Singh, H. Murayama, T. Matsui and K. Eguchi, *Electrochemistry*, 2014, **82**, 839.
27. Y. Tomita, S. Teruya, O. Koga and Y. Hori, *J. Electrochem. Soc.*, 2000, **147**, 4164.
28. M. Umeda, Y. Niitsuma, T. Horikawa, S. Matsuda and M. Osawa, *ACS Appl. Energy Mater.*, 2020, **3**, 1119.
29. S. Jia, S. Matsuda, S. Tamura, S. Shironita and M. Umeda, *Electrochim. Acta*, 2018, **261**, 340.
30. S. Pérez-Rodríguez, M. Corengia, G. García, C. F. Zinola, M. J. Lázaro and E. Pastor, *Int. J. Hydrogen Energy*, 2012, **37**, 7141.
31. S. Shironita, K. Karasuda, M. Sato and M. Umeda, *J. Power Sources*, 2013, **228**, 68.
32. A. J. Bard, R. Parsons and J. Jardan, *Standard Potentials in Aqueous Solution*, Marcel Dekker, Inc., New York and Basel, 1985.
33. Y. Hori, H. Wakebe, T. Tsukamoto and O. Koga, *Electrochim. Acta*, 1994, **39**, 1833.
34. S. Trasatti and O. A. Petrii, *Pure & Appl. Chem.*, 1991, **63**, 711.
35. S. Shironita, K. Sato and M. Umeda, *Electrocatalysis*, 2018, **9**, 213.
36. M. Umeda, Y. Yoshida and S. Matsuda, *Electrochim. Acta*, 2020, **340**, DOI: 10.1016/j.electacta.2020.135945.
37. M. Jitaru, D. A. Lowy, M. Toma, B. C. Toma and L. Oniciu, *J. Appl. Electrochem.*, 1997, **27**, 875.
38. K. P. Kuhl, E. R. Cave, D. N. Abram and T. F. Jaramillo, *Energy Environ. Sci.*, 2012, **5**, 7050.
39. R. Kortlever, J. Shen, K. J. P. Schouten, F. Calle-Vallejo and M. T. M. Koper, *J. Phys. Chem. Lett.*, 2015, **6**, 4073.
40. W. Zhang, Y. Hu, L. Ma, G. Zhu, Y. Wang, X. Xue, R. Chen, S. Yang and Z. Jin, *Adv. Sci.*, 2018, **5**, 1700275.